HHS Public Access

Author manuscript

Opt Lett. Author manuscript; available in PMC 2024 February 22.

Published in final edited form as:

Opt Lett. 2023 September 01; 48(17): 4578–4581. doi:10.1364/OL.490096.

Pulse-sampling fluorescence lifetime imaging: evaluation of photon economy

Xiangnan Zhou,

Julien Bec,

Katjana Ehrlich,

Alba Alfonso Garcia,

Laura Marcu*

Department of Biomedical Engineering, University of California, Davis, California 95616, USA

Abstract

This Letter presents an experimental study comparing the photon rate and photon economy of pulse sampling fluorescence lifetime imaging (PS-FLIm) with the conventional time-correlated single photon counting (TCSPC) technique. We found that PS-FLIm has a significantly higher photon detection rate (200 MHz) compared with TCSPC (2–8 MHz) but lower photon economy (4–5 versus 1–1.3). The main factor contributing to the lower photon economy in PS-FLIm is laser pulse variability. These results demonstrate that PS-FLIm offers 25× faster imaging speed than TCSPC while maintaining room light rejection in clinical settings. This makes PS-FLIm a robust technique for clinical applications.

Fluorescence lifetime imaging is a powerful minimally invasive imaging technique that provides tissue biochemical composition information, with broad applications from basic science to clinical research [1]. Fluorescence lifetime detection is ratiometric and thus robust to changes in fluorescence excitation-collection geometries and non-uniform tissue illumination. The most common measurement principle for the fluorescence lifetime is time-correlated single photon counting (TCSPC). TCSPC is a statistical method that detects single fluorescence photons and their arrival times with respect to a reference signal from the light source. The fluorescence decay is recorded as a histogram of thousands of precisely time-registered single photons. Hence, for practical application in the operating room (OR), it requires a light source with a high repetition rate (usually 20 to 80 MHz) to accumulate enough photons to measure the fluorescence decay with precision in a timely manner (< 1 s) [2]. TCSPC provides the significant advantage of being close to ‘shot-noise’ limited, i.e., the signal-to-noise ratio (SNR) of TCSPC approaches the limits imposed by the quantized nature of light. TCSPC is the *de facto* standard for fluorescence lifetime imaging microscopy (FLIM) due to its high photon efficiency, high temporal resolution, and its ability to operate with low-energy pulses (~nJ). However, two main drawbacks currently limit the transition of TCSPC-based systems into the OR: 1) the inherently slow acquisition times due to the

* lmarcu@ucdavis.edu .

Disclosures. The authors declare no conflicts of interest.

low photon arrival rate of below 10% of the excitation repetition rate, limited by the detector dead time and the restriction of the time-to-digital converters to count only one photon per cycle [3], and 2) the influence of background/room light. While the former can be addressed by employing single photon avalanche diodes (SPADs) with sub-ns dead times [4] or SPAD arrays with time gating [5] or on-chip per-pixel histogramming [6], the latter remains challenging. Room light, uncorrelated to the reference signal, is detected as a constant background in addition to the detector's dark counts and hence leads to worsened photon efficiency, lifetime estimation error, and reduced lifetime contrast [2,7]. In a clinical setting, the elimination of ambient room light can potentially disrupt the clinical workflow. A recent approach suggested that synchronous external illumination could address this shortcoming and facilitate future implementations of TCSPC-based technology in clinics [8,9]. However, the current instrumentation is limited to a frame rate of 50 Hz to avoid the stroboscopic effect of a blinking source, and its compatibility with existing OR light sources is also a concern.

An alternative lifetime measurement principle successfully adopted into the OR workflow is the 'single-shot' analog pulse-sampling FLIm (PS-FLIm) (also referred to as transient recording). In PS-FLIm, a large number of fluorescence photons are generated by a short (sub-ns) and intense (~0.1–10 μJ) excitation pulse and detected by a high-bandwidth photodetector [10]. The analog electrical transient signal can be captured with a fast digitizer with a temporal resolution of tens of picoseconds, allowing fast and direct recordings (~ a few μs) of fluorescence decay. The large number of fluorescence photons detected per excitation pulse leads to fast data acquisition and ensures that background illumination is unlikely to adversely impact the fluorescence signal. This makes PS-FLIm favorable for clinical applications that require fast acquisition times.

This Letter describes two critical system performance parameters, namely the photon detection rate and the photon economy, of a multispectral PS-FLIm system used in clinical research studies [11]. These performance parameters are compared with conventional single-detector TCSPC systems and advanced TCSPC systems using a SPAD array. In brief, the multispectral PS-FLIm system uses a pulsed 355 nm laser for fluorescence excitation (STV-02E-140, TEEM Photonics, France). An optical fiber probe (FG365UEC, Thorlabs Inc., NJ) delivers the excitation light to the sample. The fluorescence signal from the sample is collected by the same fiber probe, spectrally resolved in three channels, and detected by three APD modules (APD430A2-SP1, Thorlabs, NJ). The resulting electrical transient signal is recorded by three high-speed digitizer channels (PXIe-5162, National Instruments, Austin, TX) [11].

Experimental data collected during *in vivo* brain surgery was used in the computational study reported here. The number of photons detected was computed according to Fig. 1(a). To compute the total optical energy detected per measurement per channel, the area under the curve (AUC) of the detected waveform [Fig. 1(b)] was integrated over time and corrected by the TIA gain, the APD detector gain, and the APD quantum efficiency [Fig. 1(c)]. To estimate the number of photons detected per measurement per channel, the total optical energy was then divided by the average photon energy of each spectral channel.

The results show that, on average, the current clinical PS-FLIm technique detects approximately 4×10^5 photons per measurement per spectral channel and 12×10^5 photons per measurement for all three spectral channels.This is one order of magnitude higher than conventional single-channel TCSPC systems (~ 1×10^4) [8] due to the higher excitation pulse energy of PS-FLIm (~300 nJ) in comparison with TCSPC (~nJ). On average, TCSPC only detects 1 photon every 10 excitation pulses to avoid photon pileup. Taking into consideration the different laser repetition rates of PS-FLIm (460 Hz) and TCSPC (typically 80 MHz), we computed the photon rate, which is a more suitable parameter to evaluate the photon collection speed, for both techniques. The photon rate for PS-FLIm is estimated to be higher than 200 MHz for a single channel [e.g., channel 2, 470/28 nm Figs. 1(d) and 1(e)]; thus, it is 25 times higher than the 8 MHz achieved with conventional TCSPC using a single detector. For TCSPC, the laser repetition rate determines the signal period. To avoid the lifetime estimation error caused by tail cutoff, a signal period of 4–5 times the expected fluorescence lifetime is often chosen. When imaging fluorophores with long fluorescence lifetimes [i.e., lipids (8 ns) or protoporphyrin IX (16 ns)], a laser repetition rate of 40 MHz or 20 MHz is suitable, thus further reducing the photon rate of TCSPC by a factor of 2 or 4. For clinical applications where optical fibers are often utilized, the laser repetition rate has to be further reduced to allow the separation of photons generated by the optical fiber (~ 20 ns delay for 2 m of fiber) and the tissue sample [8].

PS-FLIm photon economy.

Another critical parameter of a FLIm device is the number of photons required to achieve a targeted lifetime estimation accuracy. This is characterized by the photon economy, with a figure of merit *F*-value [12] defined as $F = (\sigma/\tau) \cdot \sqrt{N}$, in which σ is the standard deviation of repeated measurements of the lifetime value τ and N is the number of detected photons. In essence, the photon economy is the ratio of the relative error of the lifetime estimate by the device under study (σ/τ) to the relative error due to pure Poissonian noise $N^{-1/2}$. For all fluorescence lifetime imaging techniques, $F \geq 1$, and the closer the value to unity, the better the performance.

The *F*-value versus the number of detected photons was studied experimentally by performing repeated measurements of Coumarin 120 dye (τ = 3.6 ns) in spectral channel 2 (470/28 nm). A neutral-density filter was used to reduce the excitation laser power while keeping the fluorescence excitation and collection geometry constant. A constant signal amplitude of 1 V was maintained by adjusting the APD gain. The total number of photons detected was computed as stated above. 1000 measurements were taken for each APD gain value, and the standard deviation of the lifetime estimation was used to compute the *F*-value. A constrained least-squares deconvolution with the Laguerre expansion (CLSD-LE) method (Laguerre order = 12, alpha = 0.916) implemented in MATLAB was used to compute the fluorescence lifetime. CLSD-LE was chosen as it enables fast estimation of decay parameters [13]. The standard deviation of the FLIm measurements, the number of photons detected in spectral channel 2, and the *F*-value are plotted in Fig. 2. It can be observed that the *F*-value achieved by PS-FLIm (in the range of 4 to 5) exceeds that of TCSPC (in the range of 1 to 1.3) [14]. This is not surprising as, unlike TCSPC, which is shot-noise

limited, PS-FLIm measurements suffer from additional noise sources, including digitizer white noise, excess noise of the APD detector, and variation of the laser pulse width.

The effect of excitation laser pulse variability.

The effect of laser pulse width variability on the PS-FLIm lifetime estimation error is of particular interest. For PS-FLIm, each recorded fluorescence waveform results from a single excitation laser pulse. Variations in laser pulse width directly contribute to the measurement uncertainty of the captured fluorescence decays. However, this variability is absent from the system's instrument response function (IRF) because only one IRF is typically recorded for PS-FLIm. As a result, variations in laser pulse width contribute directly to the lifetime estimation error. In contrast, for TCSPC, the laser pulse variability is not a significant concern for two reasons. 1) TCSPC is a statistical method; both the system IRF and the fluorescence lifetime histograms are reconstructed over thousands of excitation laser pulse cycles. Hence, the variation of the laser pulse width is captured by both the IRF and the fluorescence signal. 2) In low-pulse-energy laser diodes, which are often used for TCSPC, the laser pulse width is narrow (tens of ps) compared with that used for PS-FLIm (hundreds of ps), so its influence its negligible for fluorescence lifetime estimations in the ns regime.

In this study, the variability of the excitation laser pulse width (STV-02E-140, Teem Photonics, France) was measured using a microchannel plate photomultiplier (MCP-PMT) detector (R3809U-50, 45ps FWHM, Hamamatsu, Japan) and a fast digitizer (PXIe-5185, National Instruments, Austin, TX), as shown in Fig. 3(a). 5000 measurements were carried out. A full width at half maximum (FWHM) of 567 ps was observed, with a standard deviation of 27 ps (4.7%). The 20% to 80% rise and 80% to 20% fall times of the laser pulse were computed and visualized in a 2D histogram [Fig. 3(b)]. No correlation was observed between the rise and fall times of the laser pulse.

The effect of the observed laser pulse variability on the estimated fluorescence lifetime was also investigated using synthetic data. The measured laser pulse data cannot be used because, in addition to laser pulse width variability, it also includes various types of system noise, including but not limited to excess noise from the MCP-PMT and white noise from the digitizer. Averaging could not be performed on the measured laser pulse as that would also average out the laser pulse width variability. Therefore, 5000 laser pulses (system IRF) consisting of two half-Gaussian profiles with different rise and decay times were simulated to match the mean and standard deviation of the experimental rise and decay times. Fluorescence decays with known lifetimes of 1 to 8 ns (in 1 ns steps) were convolved with the simulated IRFs to generate simulated waveforms representing the measured fluorescence decay signal (not shown). The mean of all the simulated IRFs was used for lifetime estimation using CLSD-LE as described above. The standard deviation of the lifetime estimation as a function of the known lifetime is depicted in Fig. 3(d). The simulation results reveal that the laser pulse variability caused a lifetime estimation standard deviation of around 30 ps for the current PS-FLIm instrumentation, which accounts for 50% (std = 57 ps for $N = \sim 0.75 \times 10^5$) of the observed standard deviation in the Coumarin 120 measurements (Fig. 2). The lifetime estimation standard deviation increases with the lifetime under investigation and gradually stabilizes as the lifetime increases to higher than 7 ns.

The *F*-value of the PS-FLIm can be improved by acquiring the IRF to characterize the laser pulse variability for each lifetime measurement for future applications where improving the photon economy is required, due to either a limited photon budget or a requirement to discriminate between close lifetime values. For current clinical applications, the lifetime estimation standard deviation values of 30–60 ps are satisfactory for the typical contrast observed (0.5–2 ns) [15,16].

PS-FLIm versus TCSPC comparison.

Table 1 summarizes the key performance parameters of a clinically employed PS-FLIm system and a comparable TCSPC FLIm system using a single hybrid detector. Both systems use an optical fiber for free-hand point-scanning imaging. For PS-FLIm, a photon rate greater than 200 MHz per channel can be achieved thanks to the high number of detected photons per excitation pulse, despite the low excitation laser repetition rate of 460 Hz used for *in vivo* clinical work. This is two orders of magnitude higher than the photon rate achievable (2 MHz) for the conventional TCSPC system with 20 MHz lasers and 10% detection efficiency [8]. The photon economy of PS-FLIm (4 to 5), on the other hand, is worse than that achieved with TCSPC (1 to 1.3). However, for clinical applications, the goal is to achieve accurate lifetime measurements with the shortest data acquisition time without exceeding the safe tissue exposure limit. The combination of photon rate and photon economy ultimately determines the data acquisition speed of the imaging system. In that aspect, PS-FLIm has an edge over standard TCSPC as it has a two orders of magnitude higher photon rate but only a five times lower photon economy. Theoretically, PS-FLIm can achieve the same lifetime accuracy with 25× less time than a standard TCSPC system. Note that, currently, the laser repetition rate of our PS-FLIm system is limited to 460 Hz for clinical applications to facilitate compliance with the IEC 60825 safety standard in the case of fiber-based freehand scanning applications.

In addition, due to the large number of photons generated in the short acquisition window (typically less than 240 ns) and a low data acquisition duty cycle (240 ns/2 ms excitation laser period), PS-FLIm is relatively unaffected by room light (rejecting 99.99% of the room light), making it favorable for clinical applications. To date, we are not aware of any TCSPC-based FLIm system used *in vivo* in a surgical setting, but PS-FLIm has been successfully integrated into the workflow of head and neck cancer [17] and brain tumor [16]. However, one major concern/limitation of PS-FLIm is the use of high-energy excitation pulses. For PS-FLIm, one must carefully balance the excitation pulse energy and its spot size to comply with tissue exposure guidelines (IEC 60825–1). Thus, PS-FLIm is better suited for mesoscopic resolution in clinical applications [18].

For applications with automated sample scanning (e.g., galvanometer based), the laser repetition rate of PS-FLIm can be significantly increased without risking tissue damage, thus further increasing the photon rate. As the electronics in PS-FLIm have no dead time, the photon rate of the PS-FLIm is mostly limited by the availability of ~ns pulsed light sources with sufficient pulse energy (0.1–10 μJ). A photon rate of ~36 GHz can be easily achieved by upgrading the current instrument with a 30 kHz light source (i.e., SNV-60P-10x, TEEM Photonics, France). For TCSPC, improved photon rates can be achieved with advanced

detectors such as SPAD arrays. These utilize parallel detection by hundreds of pixels and have recently been implemented in point-like FLIM, widefield FLIM, and multi-beam FLIM [19]. A photon detection rate of 192.4 MHz was recently demonstrated with a SPAD array of 512 × 16 pixels [6]. However, the theoretical photon rate is only achievable under ideal conditions (a bright and uniform sample), and SPAD imagers are still mostly used in specialized research settings due to drawbacks such as a low fill factor (~4%), resulting in low photon collection efficiency, which is critical for clinical applications where the photon budget is limited by safe tissue exposure. Table 2 summarizes the key performance parameters of the state-of-the-art PS-FLIm and TCSPC-FLIm with SPAD arrays.

Conclusion.

In summary, we have reported the first experimental study of the photon detection rate and photon economy of PS-FLIm in comparison with conventional TCSPC. We estimated that more than 4×10^5 photons can be detected per excitation pulse per channel using PS-FLIm compared with 0.1 photons per excitation pulse for TCSPC. With an excitation laser repetition rate of 460 Hz limited by safe tissue exposure in clinical applications, a photon detection rate higher than 200 MHz per spectral channel can be achieved in biological tissue by PS-FLIm. That is two orders of magnitude higher than that of a similar conventional TCSPC system (2 MHz). We determined the photon economy of PS-FLIm to be in the range of 4 to 5, with detected photon numbers varying from 1×10^5 to 4×10^5 photons. This is higher than TCSPC (typically 1 to 1.3), but expected as PS-FLIm suffers from systematic noise, including but not limited to excess noise from the detectors, white noise from the digitizer, and excitation laser pulse width variability. The experimentally measured laser pulse variability (FWHM 567 ps ± 27 ps) results in ~30 ps of lifetime estimation variability, accounting for 50% of the lifetime standard deviation of PS-FLIm. Despite having worse photon economy, PS-FLIm can still achieve similar lifetime measurement accuracies 25× faster than conventional TCSPC due to its high photon detection rate, making it favorable for clinical applications in which the data acquisition time is constrained. In addition to the advantage in imaging speed, PS-FLIm is also less sensitive to background light because of a very low duty cycle, strengthening its position as a promising minimally invasive tool for clinical applications, including surgical guidance.

Funding.

National Institutes of Health (P41EB032840, R01CA187427, R01HL157712, R01CA250512).

Data availability.

Data underlying the results presented in this paper are not publicly available at this time but may be obtained from the authors upon reasonable request.

REFERENCES

1. Datta R, Gillette A, Stefely M, and Skala MC, J. Biomed. Opt 26, 070603 (2021). [PubMed: 34247457]
2. Kollner M and Wolfrum J, Chem. Phys. Lett 200, 199 (1992).

3. Becker W, Advanced Time-Correlated Single Photon Counting Techniques (Springer Science & Business Media, 2005), Vol. 81.
4. Severini F, Cusini I, Berretta D, Pasquinelli K, Incoronato A, and Villa F, IEEE J. Select. Topics Quantum Electron 28, 1 (2022).
5. Smith JT, Rudkouskaya A, Gao S, Gupta JM, Ulku A, Bruschini C, Charbon E, Weiss S, Barroso M, Intes X, and Michalet X, Optica 9, 532 (2022). [PubMed: 35968259]
6. Erdogan AT, Walker R, Finlayson N, Krstajic N, Williams GOS, Girkin JM, and Henderson RK, IEEE J. Solid-State Circuits 54, 1705 (2019).
7. Becker W, Bigger and Better Photons: The Road to Great FLIM Results (Becker & Hickl, 2023).
8. Lagarto JL, Shcheslavskiy V, Pavone FS, and Cicchi R, J. Biophotonics 13, e201960119 (2020). [PubMed: 31742905]
9. Lagarto JL, Villa F, Tisa S, Zappa F, Shcheslavskiy V, Pavone FS, and Cicchi R, Sci. Rep 10, 8116 (2020). [PubMed: 32415224]
10. Steingraber OJ and Berlman IB, Rev. Sci. Instrum 34, 524 (1963).
11. Zhou XN, Bec J, Yankelevich D, and Marcu L, Opt. Express 29, 20105 (2021). [PubMed: 34266107]
12. Philip J and Carlsson K, J. Opt. Soc. Am. A 20, 368 (2003).
13. Liu J, Sun Y, Qi J, and Marcu L, Phys. Med. Biol 57, 843 (2012). [PubMed: 22290334]
14. Esposito A, Popleteeva M, and Venkitaraman AR, PLoS One 8, e77392 (2013). [PubMed: 24204821]
15. Marsden M, Weyers BW, Bec J, Sun T, Gandour-Edwards RF, Birkeland AC, Abouyared M, Bewley AF, Farwell DG, and Marcu L, IEEE Trans. Biomed. Eng 68, 857 (2021). [PubMed: 32746066]
16. Noble Anbunesan S, Alfonso-Garcia A, Zhou X, Bec J, Lee HS, Jin LW, Bloch O, and Marcu L, J. Biophotonics 16, e202200291 (2022). [PubMed: 36510639]
17. Duran-Sierra E, Cheng S, Cuenca R, Ahmed B, Ji J, Yakovlev VV, Martinez M, Al-Khalil M, Al-Enazi H, and Jo JA, Biomed. Opt. Express 13, 3685 (2022). [PubMed: 35991912]
18. Alfonso-Garcia A, Bec J, Weyers B, Marsden M, Zhou X, Li C, and Marcu L, J. Biophotonics 14, e202000472 (2021). [PubMed: 33710785]
19. Bruschini C, Homulle H, Antolovic IM, Burri S, and Charbon E, Light: Sci. Appl 8, 87 (2019). [PubMed: 31645931]

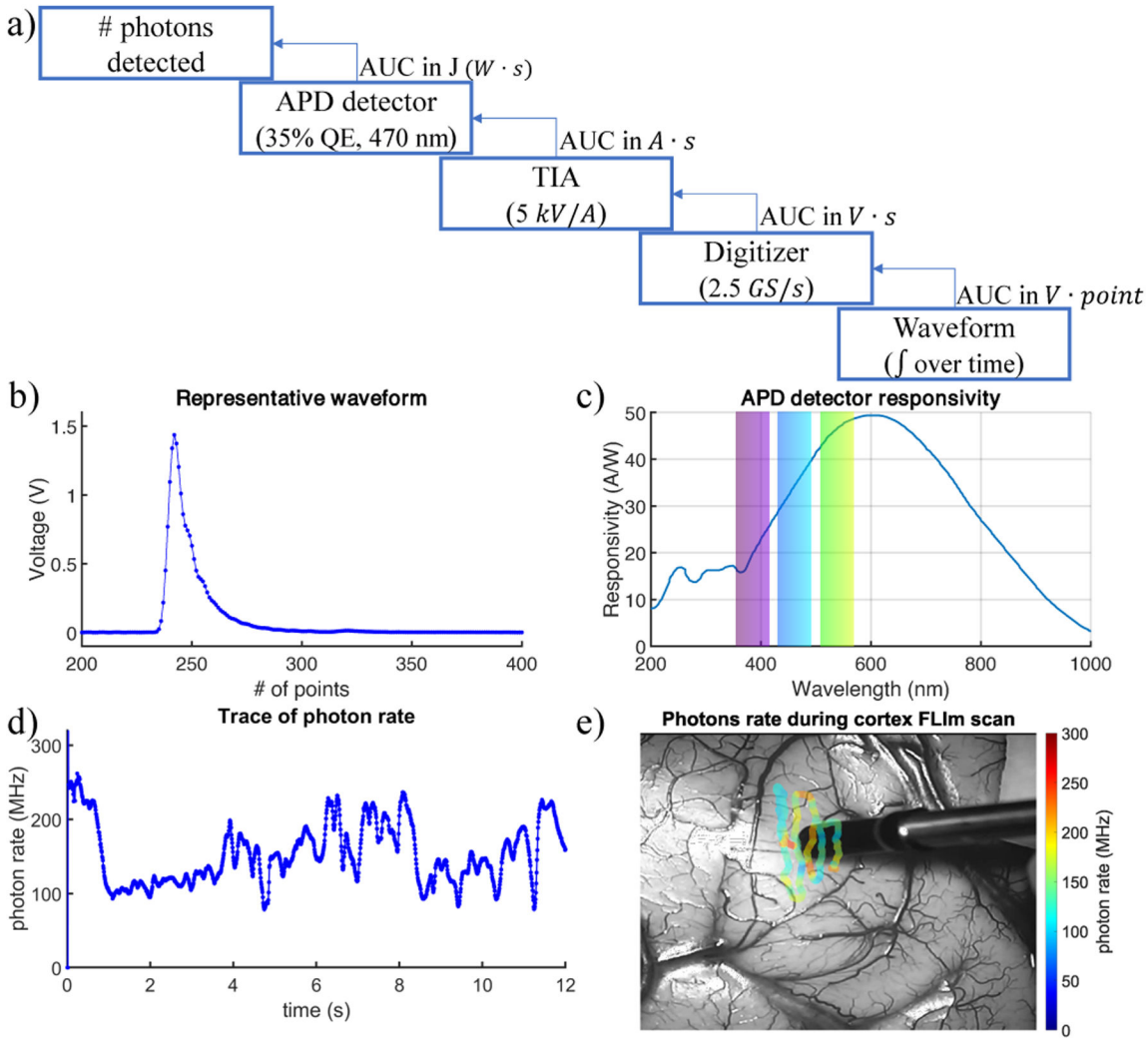

Fig. 1.

Estimation of the photon rate by the pulse sampling technique. (a) Steps used to calculate the number of photons detected for each excitation pulse. (b) Representative waveform. (c) Typical APD (e.g., blue-enhanced) detector responsivity. Highlighted areas represent the wavelength ranges of the three spectral channels in the multispectral PS-FLIm system. (d) Trace of the photon rate for spectral channel 2 (470/28 nm). (e) Overlay of the photon rate during *in vivo* FLIm measurement of cortex tissue.

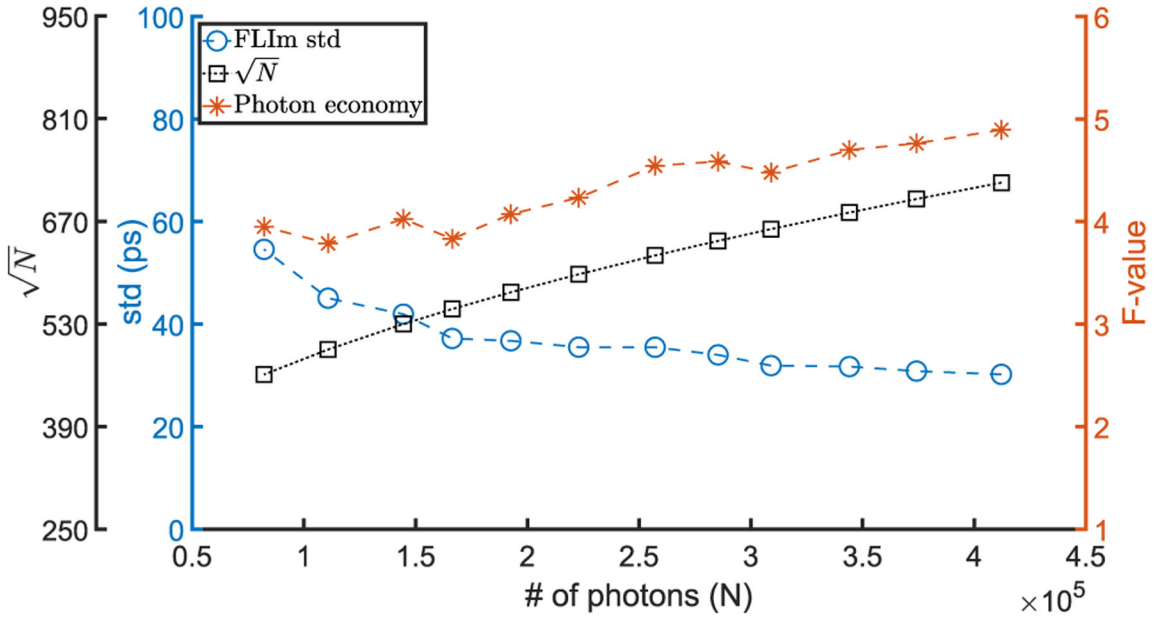

Fig. 2.

Photon economy (*F*-value) of the PS-FLIm versus the number of photons detected per measurement. The measured fluorescence lifetime standard deviation (std, n = 1000) and the estimated number of photons [sqrt(*N*)] are also plotted. Note: the experiments were performed on Coumarin 120 in ethanol solution.

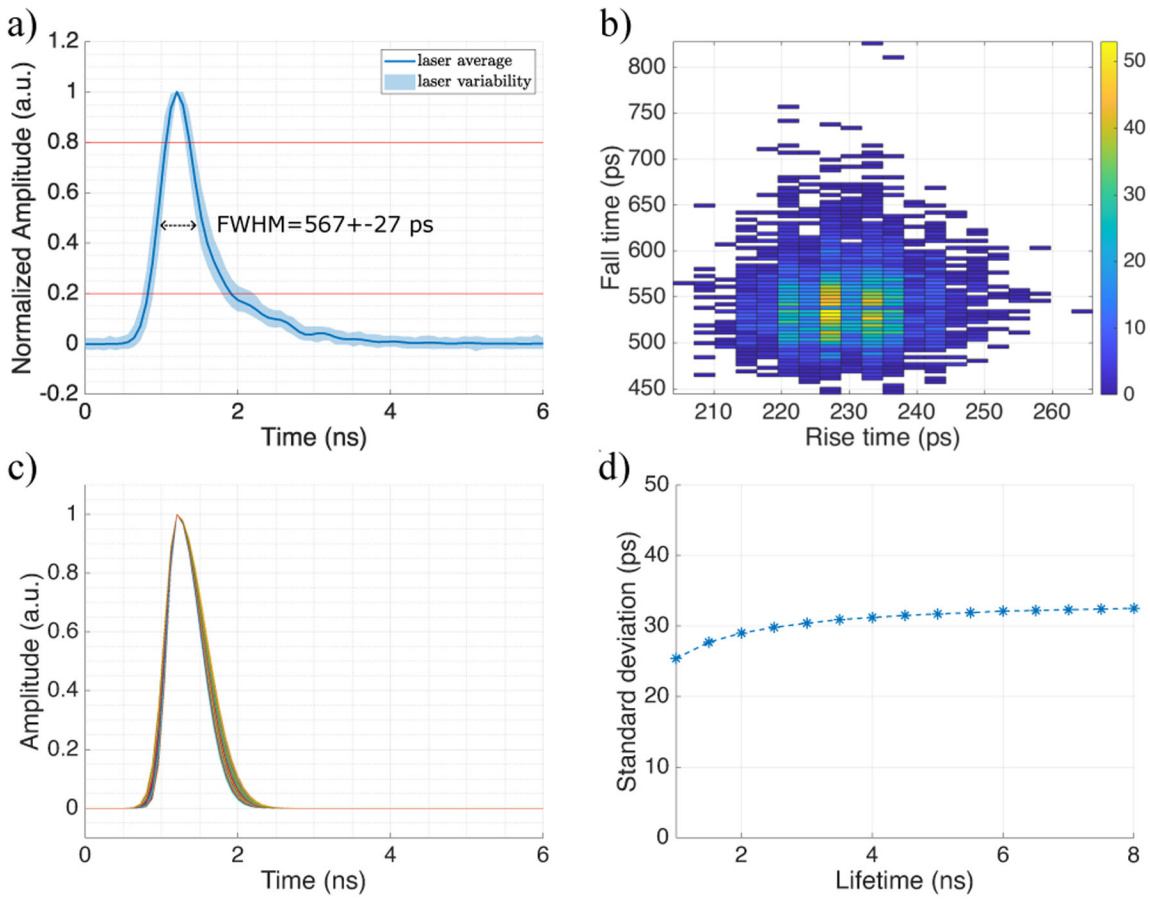

Fig. 3.

Effect of laser variability on the computed lifetime standard deviation for PS-FLIm. (a) Average (solid line) and standard deviation (shaded area) derived from 5000 laser pulse measurements after peak normalization and temporal alignment. (b) 2D histogram of the rise and fall times from 20% to 80% [as indicated in (a)] of the laser pulse measurements. (c) Simulated IRF (laser pulse) consisting of a Gaussian profile with different rise and decay times matching the mean and standard deviation of the experimental rise and decay times. (d) Computed lifetime standard deviation caused by the laser pulse for different average lifetime values.

Table 1.

Key Parameters of PS-FLIm and TCSPC for Clinical Application (Single Channel)

	Pulse Sampling	TCSPC
Laser repetition rate	460 Hz [11]	20 MHz [8]
Photon rate per pulse	$>4 \times 10^5$	0.1
Photon rate (s^{-1})	> 200 MHz	2 MHz
Photon economy	4–5	1~1.3 [14]
Acquisition duty cycle	0.01% (240 ns/pulse)	100%
Background rejection	Yes (99.99%)	No

Table 2.

Key Parameters of State-of-the-Art PS-FLIm and TCSPC (Multi-Channel)

	Pulse Sampling	SPAD Array
Laser repetition rate	30 kHz	80 MHz
Photon rate per pulse	~4×10^5	0.1
# of channels/pixels	3	Up to ~8k
Photon rate (s^{-1})	~36 GHz	192.4 MHz [6]
Photon economy	4–5	1~1.3 [14]
Acquisition duty cycle	0.7% (240 ns/pulse)	100%
Background rejection	Yes (99.3%)	No